

## **Analysis of flat glass deposited thin film made from aluminium doped zinc oxide (AZO)**

G. Osayemwenre<sup>a,\*</sup>, F. Inambao<sup>b</sup>, O. A. Osibote<sup>a</sup>

<sup>a</sup>*Department of Mathematics and Physics, Faculty of Applied Sciences, Cape Peninsula University of Technology, Cape Town, South Africa*

<sup>b</sup>*Department of Mechanical Engineering, Faculty of Engineering, University of KwaZulu-Natal, Durban, South Africa*

Doped aluminium zinc oxide (Al doped ZnO/AZO) thin films that were synthesised on glass and nanostructured with cadmium substrates were allowed to degrade over a period of two years in a controlled environment. The films were placed in airtight containers for eighteen months and later placed in plastic containers for four months at room temperature. This environment was able to allow slight damping at times to accelerate the physical degradation process. The evolution of transparent conductive oxide (TCO) like aluminium doped zinc oxide (AZO) has been a welcome development in solar cell production. But it quickly deteriorates which is a drawback in its application. In this study, each film was doped with the same Al concentration but in different mediums such as cadmium, nitrogen, silver and argon (Cd, N<sub>2</sub>, Ag, Ar). To investigate the optical performance, the transmittance of each film was studied. An average transmittance of above 65 % was observed. The optical properties in these films were varied by the different mediums which are cadmium, nitrogen, silver and argon (Cd, N<sub>2</sub>, Ag, Ar). It was observed that the transmission over the visible range varied as the wavelength increased. This change happens because of free carriers coupling to the electric field leading to high reflection. Therefore, the simplest way to quantify the degree of degradation was to investigate the optical properties such as the transmission between layers. The micro-structure of these thin films were evaluated using scanning probe microscopy (SPM) to demonstrate degradation. Finally, the morphological and elemental compositions were analysed with scanning electron microscopy (SEM) and energy-dispersive X-ray spectroscopy (EDX).

(Received June 18, 2021; Accepted November 10, 2021)

**Keywords:** Aluminium doped zinc oxide (AZO), Transparent conductive oxide (TCO), Degradation, Energy diffraction X-ray (EDX).

### **1. Introduction**

Transparent conductive oxides (TCOs) such as aluminium doped zinc oxide (AZO) are used in electronic, transistor and solar industries due to their optoelectronic ability. They function as components in optoelectronic and solar devices [1-3]. TCOs are simplified metallic oxide materials with the ability to conduct electric current and still retain their optical transmission power [4]. Every TCO is known by two important features, namely, good transmission of about 80 % and low resistivity of around  $10^{-3}$  ohm<sup>-cm</sup> to  $10^{-4}$  ohm<sup>-cm</sup> [5-6]. Indium tin oxide (ITO) exhibits the above named two features too [7-8], but AZO has an added advantage which is a flexible wide band gap. Furthermore, unlike AZO, ITO has high production costs, is time consuming, and is limited in nature. Thus, ZnO has shown itself to be a better candidate. In the early stage of optoelectronics industry ITO was the most commonly used material for optoelectronic material and for thin film in some organic light-emitting diodes, antistatic coatings, and solar cells. However, its scarcity in nature and huge production costs have led to its replacement with the more economic TCOs such as ZnO. ZnO is abundant in nature and has cheap production costs. However, ZnO is less attractive as a conductive oxide because it is highly prone to degradation

---

\* Corresponding author: osayemwenreg@cput.ac.za

compared to ITO [8]. In the preparation of AZO, usually the n-material is doped with a group III metal in order to increase the carrier concentration which indirectly lowers the material resistivity. Other qualities of ZnO include its optical band gap of 3.3 eV, good electrical and optical properties, low level of toxicity and high chemical stability [1, 3-4, 8].

Research interest in ZnO keeps growing because of its unique qualities which can easily be increased through modification. This modification process is crucial in developing state of the art transparent electrodes required in the electronic industry for touch screens, LCDs, plasma display panels (PDPs), and solar cells applications [8-10]. Recently, impurity-doped ZnO [10-11] has been produced which shows better electrical and optical features for TCO and is believed to be a suitable candidate for replacement of ITO. Previous work by [5, 11] shows that n-type ZnO exhibits high binding energy of the order of 60 MeV coupled with good chemical and thermal stability. Based on this, ZnO can be doped to increase its properties such as stability, optical and electronic properties. ZnO doped with Al (AZO) has shown an increase in free charge carriers of larger optical bandgap compared to undoped ZnO[12].

The attempt to completely replace ITO in optoelectronics devices requires more research. The more that TCO film with wide band gap is able to give low resistance and great transparency in the visible light region, the better [13]. TCO optical band gap values of 3.5 to 4.06 have been reported in literature as good values. The TCO studied in this study is Al doped ZnO/AZO. The extrinsic donors of doped ZnO films are quite stable compared to the intrinsic donors as a result of negative charges. The enhancement of its electrical power is linked to its Al<sup>3+</sup> ions in substitution sites of Zn<sup>2+</sup> ions as well as the aluminium interstitial atoms [13-14]. The electrical efficiency also depends on its oxygen vacancies and zinc interstitials as reported by Tanusevskia et al. [14]. This work is primarily focused on the analysis of long-term stability effects on the morphology, chemical and optical transmission to access the structure and the quality of AZO thin films. Such an investigation is essential to achieve a better understanding of variation in performance over a long period of time. As degradation continues, it affects the roughness and thickness of the AZO thin film, and this may lead to inhomogeneity in its morphology. Some authors have proved that the thickness of AZO is related to its stability [10, 15], therefore a change in its thickness will also affect the transmission which is detrimental to its performance.

## **2. Baseline characterisation and sample preparation**

The samples were subjected to initial characterisation 24 hours after fabrication, to analyse their structural and morphological properties. Film roughness, interface roughness, thickness deposited, and thickness were measured using X-ray reflectometry (XRR) and scanning probe microscopy (SPM). Table 1 shows the initial measurements of film roughness and interface roughness.

*Table 1. Baseline readings.*

Deposition thickness (nm)	XRR thickness (nm)	Film roughness (nm)	Interface roughness (nm)	Film roughness (Ra) (nm)	Rq roughness (nm)
AZO/Cd-300	307+13	3.35+0.1	3.29+0.6	4.50	3.21
AZO/Ag-300	307+13	3.35+0.1	3.29+0.6	3.83	3.19
AZO/N <sub>2</sub> -300	307+13	3.35+0.1	3.29+0.6	3.47	3.20
AZO/Ar-300	307+13	3.35+0.1	3.29+0.6	3.51	3.10

The first stage of preparation was to get a section of the TCO material cut out and cleaned using standard cleaning methods to eliminate any possible contamination using distilled water and compressed air. Immediately after the sample was cleaned, it was placed on a holding stab before it was introduced into the SPM device. The AZO thin films used in this research were laboratory made.

### **3. Experimental Techniques**

#### **3.1. Thin film topography**

Scanning electron microscope (SEM) and atomic force microscope (AFM) were used for the morphology. The scanning probe microscope (SPM) used was a Bruker Dimension ICON instrument with an amplifier current range of 1 pA to 1  $\mu$ A. The morphology characterisation of AZO thin films was done with a SEM and complimented by SPM. The operating voltage and current were maintained for all the analysed samples. All measurements were made under ambient conditions of 20 °C temperature and 50 % to 60 % humidity. The addition of super-sharp silicon probes of 2 nm nominal radius helped to obtain higher-resolution topography images. The AZO conductive thin films analysed were AZO/Cd, AZO/N<sub>2</sub>, AZO/Ag, and AZO/Ar. These AZOs were all grown by the same technique, which is chemical vapour deposition but in different medium such are cadmium, nitrogen, silver and argon. Using an SPM in non-contact mode, the morphology and the structural properties of the AZOs were studied. In all measurements, a conductive Pt-coated tip with a resonant frequency of 70 kHz spring constant 2N/m was used. This technique was used to acquire the topography of the sample surface. Lastly the chemical composition was analysed with energy-dispersive X-ray spectroscopy (EDX).

#### **3.2. Optical measurement**

The optical measurements of Al doped ZnOs were measured by UV/VIS/NIR 3700 double beam Shimazu spectrophotometer in the range of 300 nm to 2500 nm. The device irradiated the sample with selected photons wavelengths of beam intensity to produce transmissions. Through the help of a spectrophotometer, only selected wavelength photons were released. These photons were classified into two according to their energies. When illuminated the sample absorbed the more energetic photons whose energy exceed the band gap (Eg) but transmit the one with less energies than the band gap.

## **4. Results**

#### **4.1. Surface morphology and composition analysis of doped AZO thin films**

The SEM microgram of all the Al doped films are shown in Figure 1 (a) to (d). The figure images are threadlike, rootlike and circular with semi wurtzite structure. The particle size varies between 5 nm and 50 nm [16]. The rise in size above 25 nm is linked to surface defects caused by oxidation due to long degradation effects. It can see that the surface morphology of all samples shows that the thin films were crack free, with uniform texture in most regions while the nano fibre seen in one of the samples was found to be poorly structured due to degradation. The shape, structure and size of these AZO were determined from SEM analysis. The micrographs indicate a nano-shape in only one of the images, while the others are slight spherical and threadlike but with uniform distribution in most areas of the images. The SEM images illustrate that using different doping precursors does not affect only the performance but also the thin film size and shape. It can be seen from the SEM images that using nano structure substrates, the zinc oxide molecules grew slowly into small nano spherical structures (AZO/N<sub>2</sub>) with a uniform hole-like shape. The ZnO/Cd particles have some flowering particles by replacing flat glass substrate with nanostructure. The size of the particles are smaller than the 47.27 nm reported by Vasile et al. [18]. In the case of AZO/Ag, the zinc oxide molecules are slightly spherical with inhomogeneous shape, which appears to accumulate around the middle. For ZnO/Cd and AZO/Ar the images are characterised by threading structure. The presence of web-like image with a few threadlike structures in AZO/Ar and a large diameter compared to what is observed in AZO/Cd was observed. On the other hand, in a nitrogen atmosphere, the agglomeration observed is due to polarity together with electrostatic attraction of ZnO particles, unlike what was presented by Divya et al. [17].

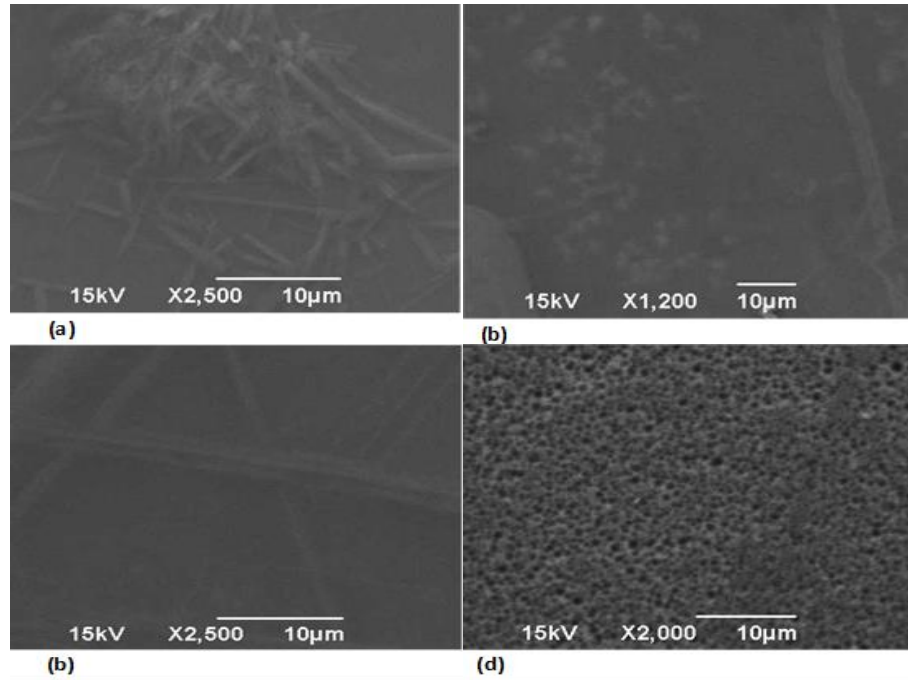


*Fig. 1. SEM analyses of ZnO sample doped with Al (a) AZO/Cd (b) AZO/Ag (c) AZO/Ar and (d) AZO/N<sub>2</sub>.*

#### 4.2. Scanning probe microscope (SPM) analysis

The SPM surface images of different AZO thin films deposited on flat glass substrates and a nanostructure substrate are shown in Figure 2. SPM images are vital in characterising the morphology and roughness of thin film surfaces through root means square (RMS). Also possible is grain size evaluation. Figure 2(a) and (b) show the SPM images of AZO thin films. The images confirmed changes in the surface morphological features as the scanned area increased. The inhomogeneity of the thin films surface morphology have various degrees of variation. Some of the samples' structures are seen to be well distributed in some areas while not in others, judging from their surface roughness. The morphology of some of the samples exhibit small granular structures, with height and width changes to some extent. Their surface morphologies are characterised by different degrees of granular structure. Figure 2 (a) to (d) show SPM images of the different AZO thin films used for SEM in Figure 1 (a) to (d).

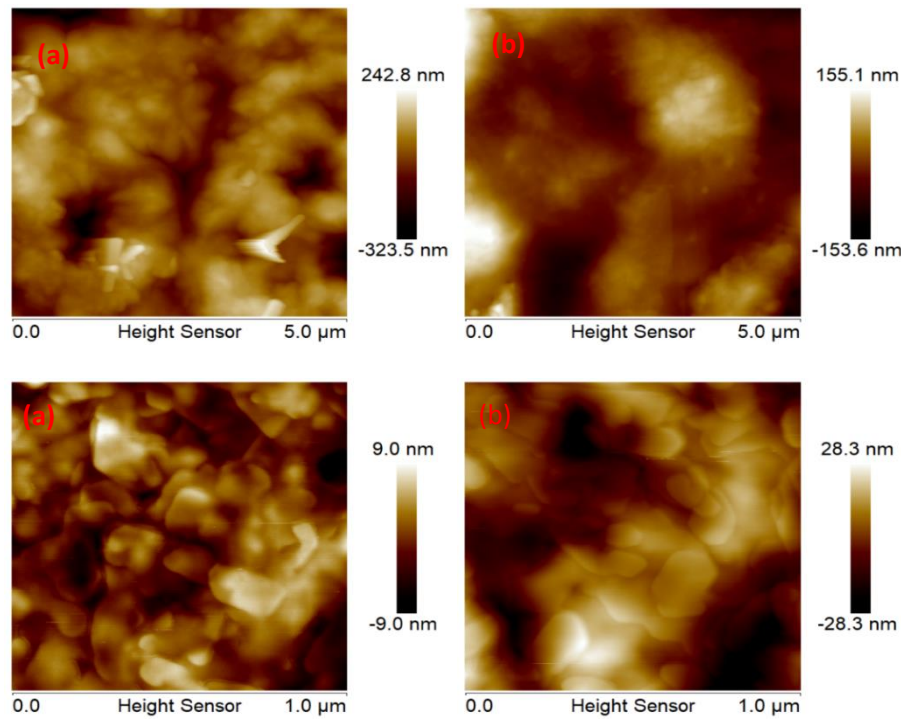


*Fig. 2. (a) 2-D top view SPM image of the AZO/Ag, AZO/Ag, AZO/Ar (nona substrate) and AZO/N<sub>2</sub> thin film grown on flat glass substrates.*

The SPM images show that AZO/Cd, AZO/Ag, AZO/Ar and AZO/N<sub>2</sub>, thin film surfaces differ in terms of structures and voids. The image in Figure 1(b) shows that the AZO/Ar film has the lowest roughness while the highest roughness is AZO/Cd. From these images it is clear that the thin films exhibit surface morphological features of a large roughness, far more than what was observed in table 1.

#### 4.3. Chemical composition analysis of doped AZO thin films

The surface morphology ZnO after two years in different mediums was measured simultaneously with EDX for elemental analysis. The chemical composition indicates that Zn L $\alpha$ , Zn K $\alpha$ , Al K $\alpha$ , O<sub>2</sub> K $\alpha$ , C K $\alpha$ , Si K $\alpha$  are seen to be common to all the four samples. The Zn L $\alpha$  peaks in 1.1 keV, 1.49 keV, 0.56 keV, 0.28keV, 1.78keV could be observed in the spectra which agree with the literature [18]. The percentage compositions are given in Figure 3. The quantity of oxygen is hard to pin to O K $\alpha$  due to the presence of SiO substrate [19]. The EDX spectra revealed the presence of Zn and Al situated in the right phase and confirm the levels of purity with the exception of O. Table 2 presents the elemental analysis of each sample and the percentage compositions. The results show that there is a slight impurity in some samples compared to others and that the quantity of Zn, Al and O ion are proof of metal oxide in the composite.

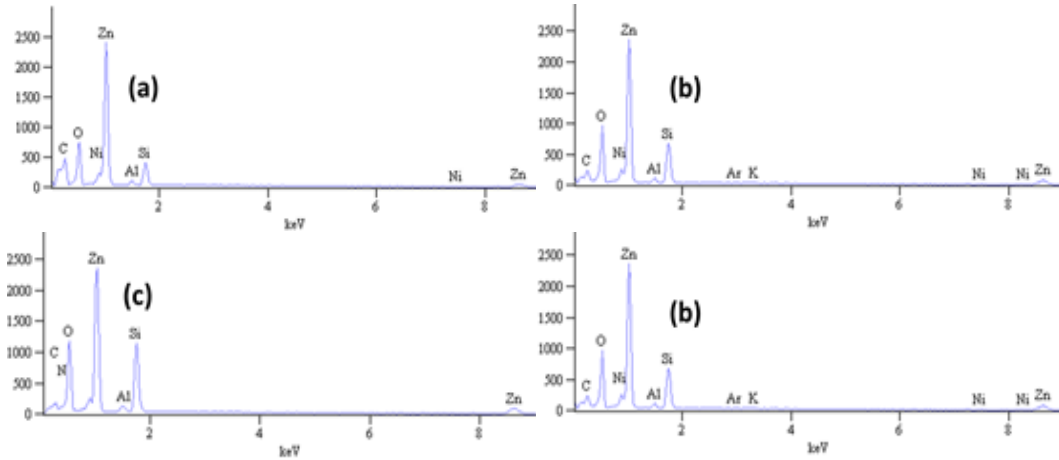


*Fig. 3. Elemental analysis of ZnO samples doped with Al (a) AZO/Cd (b) AZO/Ag (c) AZO/Ar and (d) AZO/N<sub>2</sub>*

*Table 2 Elemental composition of Al doped Zinc oxide thin film in different substance medium.*

Element	Sample			
	ZnO/Cd	ZnO/Ag	ZnO/Ar	ZnO/N <sub>2</sub>
C	10	2.05	8.02	6.53
O	32.40	36.10	20.19	22.12
Al	1.39	2.76	1.40	1.46
Si	23.55	14.57	13.91	19.60
Ar	-	-	0.29	-
Ni	0.23	0.33	-	-
Zn	30.88	42.59	56.19	50.12
Ag	-	1.59	-	-
Cd	0.57	-	-	-
N		-		0.18

#### 4.3. Optical analysis

The optical properties were observed from Fourier transform infrared (FTIR) spectroscopy and the results are presented in Figure 4. In this study optical investigation was limited to transmittance.

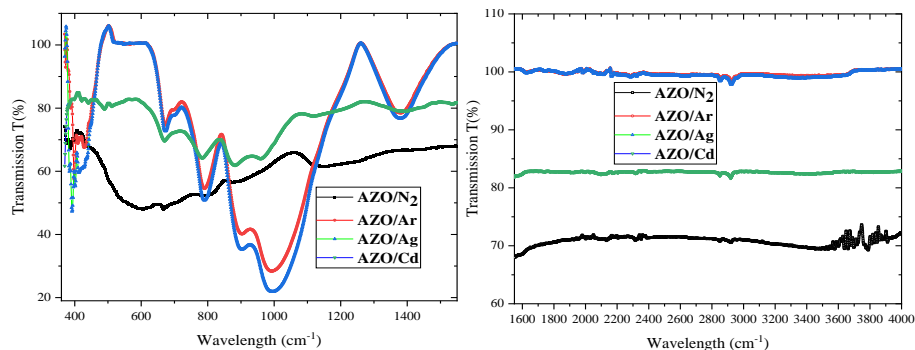


*Fig. 4. FTIR spectra of AZO doped with different substances in the wavelength of a) 380 cm<sup>-1</sup> to 1550 cm<sup>-1</sup>, b) 1550 cm<sup>-1</sup> to 4000 cm<sup>-1</sup>.*

FTIR studies of four different AZO thin films are shown in Figure 4. The infrared studies were carried out to determine the purity, nature of the AZO particles and optical performance. The first observation is the similarity in the optical performance and bonds present in ZnO/Cd and ZnO/Ar. The FTIR is divided into two based on wavelength. In Figure 4(a), the peaks that appear at  $600\text{ cm}^{-1}$  represent Zn–O stretching, while  $600\text{ cm}^{-1}$  and  $450\text{ cm}^{-1}$  correspond to deformation vibration. FTIR of AZO was performed with total reflection mode. Figure 4(a) and Figure 4(b) show the spectra for ZnO/Cd, ZnO/Ag, ZnO/ $\text{N}_2$ , and ZnO/Ar in the range of  $360\text{ cm}^{-1}$  to  $1600\text{ cm}^{-1}$  and  $1600\text{ cm}^{-1}$  to  $4000\text{ cm}^{-1}$  respectively. In Figure 4a, peaks around  $380\text{ cm}^{-1}$  to  $530\text{ cm}^{-1}$  are characteristic of stretching vibrational modes of Zn–O–Zn designated to the defected ZnO presence at room temperature [13]. The peaks observed around  $400\text{ cm}^{-1}$  to  $700\text{ cm}^{-1}$  are linked to ZnO stretching modes [21]. The presence of hydroxyl group of  $\text{H}_2\text{O}$  molecules around  $1626\text{ cm}^{-1}$  peak in slight quantity excluding AZO/ $\text{N}_2$  means lack of water molecule. The peaks between  $1010\text{ cm}^{-1}$  and  $1118\text{ cm}^{-1}$  are believed to be C–O–C and O–H bonds resulting from C–OH groups deformations [22]. A wide peak can be seen in AZO/ $\text{N}_2$  at around  $3471\text{ cm}^{-1}$ . This can be assigned to O–H stretching bond vibrations from  $\text{H}_2\text{O}$  molecules at the surface of Al doped ZnO particles [23-24]. A small peak at  $2927\text{ cm}^{-1}$  and  $2853\text{ cm}^{-1}$  can be observed in all the samples because of C–H stretching vibrations mode. The peak at  $890\text{ cm}^{-1}$  in ZnO/Cd and ZnO/Ar is due to slight C–O–C–O vibrations [25]. The peaks at  $756\text{ cm}^{-1}$  to  $789\text{ cm}^{-1}$  in all the samples are the result of crystal structure and infra-red bond intensities of different carbonate [26]. The fact that the peaks are low mean that the impact on the thin films are less effective. The optical performance of each thin film can be judged from the FTIR, with AZO/Cd and AZO/Ar having similar peaks and slightly different intensity at around  $600\text{ cm}^{-1}$  to  $1300\text{ cm}^{-1}$ . AZO/ $\text{N}_2$  has the lowest transmission followed and AZO/Cd or AZO/Ar with the highest transmission. The high performance of AZO/Ar can be attributed to its nano structure.

## 5. Conclusion

In this study, SPM measurements of AZO thin films were carried out with different doping materials on flat glass and nanostructure substrates. The grain and microstrains observed varied with AZO/Cd having the highest and AZO/Ar the lowest value. This means that AZO/ $\text{N}_2$ , and AZO/Ar are better candidates for electronic devices. The various thin films had film thickness and interface roughness after degradation, increased for AZO/Cd, AZO/ $\text{N}_2$ , AZO/Ag and AZO/Ar. The results revealed that roughness along with the average grain size of all the samples (films) rose with time and the use of various doping materials offered extra stability to the samples. Micro-structural and element composition analyses of four different AZOs were performed by SEM-SPM and EDX methods. The FTIR spectra shows that Zn distribution in each of the Al doped films was not uniform. An increased Al concentration in randomly distributed areas with about  $10\text{ nm}$  diameter was observed in the films. A more uniform distribution of Zn was observed in the films with nanostructure plate. The FTIR spectra revealed the formation of several bonds, including the Zn–O bond in all samples and the Al–O bond in the AZO samples.

## Acknowledgements

The authors would like to express their gratitude to the following organizations: UNISA, UKZN and Cape Peninsula University of Technology, South Africa for the postdoctoral fellowship funding.

## References

- [1] K. Ellmer, A. Klein, B. Rech, editors, New York: Springer; Springer Series in Materials Science, 104 (2008).
- [2] D. S. Ginley, H. Hosono, C. Paine, editors, Handbook of transparent conductors. New York: Springer; 2010.
- [3] H. Liu, V. Avrutin et al., *Superlattices and Microstructures* **53**(3), 4840 (2010).
- [4] E. P. da Silva, M. Chaves, S. F. Durrant, P. N. Lisboa-Filho, J. R. R. Bortoleto, *Materials Research* **17**(6), 1384 (2014).
- [5] K. Ellmer, A. Klein, B. Rech, editors, New York: Springer; Springer Series in Materials Science, 104 (2007).
- [6] H. Liu, V. Avrutin, N. Izyumskaya, *Superlattices and Microstructures* **48**(5), 458 (2010).
- [7] H. Zhu, Y. Mai, M. Wan, J. Gao, Y. Wang, T. He et al. **539**, 284 (2013).
- [8] A. Sharmin, S. Tabassum, M. S. Bashar, Z. H. Mahmood, *Journal of Theoretical and Applied Physics* **13**, 123 (2019).
- [9] D. C. Plain, H. Y. Yeom, B. Yaglioglu, In: Crawford GP. editor. Flexible flat panel displays, Singapore: Wiley; 794, 9 (2005).
- [10] B. G. Lewis, D. C. Plain, *MRS Bulletin* **25**(8), 22 (2000).
- [11] Y. Wang, W. Zhao, M. Zou, Y. Chen, L. Yang, L. Xu, H. Wu, A. Cao, *ACS Applied Materials & Interfaces* **9**(43), 37813 (2017).
- [12] F. D. Paraguay, W. L. Estrada, D. R. N. Acosta, E. Andrade, M. Mikiyoshida, *Thin Solid Films* **350**, 192 (1999).
- [13] F. K. Mugwanga, P. K. Karimi, W. K. Njoroge, O. Omayio, *Journal of Fundamentals of Renewable Energy Applications* **5**(4), 2015.
- [14] A. Tanusevskia, V. Georgieva, *Applied Surface Science* **256**(16), 2010.
- [15] K. Haga, M. Kamidaira, Y. Kashiwaba, T. Sekiguchi, H. Watanabe *Journal of Crystal Growth* **214**, 77 (2000).
- [16] P. S. Shewale, G. L Agawane, S. W. Shin, A. V. Moholkar, J. Y. Lee, J. H. Kim, M. D. Uplane, *Sensors and Actuators B* **177**, 695 (2013).
- [17] M. J. Divya, C. Sowmia, K. Joona, K. P. Dhanya, *Research Journal of Pharmaceutical, Biological and Chemical Sciences* **4**(2), 1137 (2013).
- [18] E. Vasile, R. Plugaru, S. Mihaiu, *A. Romanian Journal of information Science and Technology* **14**(4), 346 (2011).
- [19] M. E. Fragala, G. Malandrino, *Microelectronics Journal* **40**, 381 (2009).
- [20] S. Chakma, J. B. Bhasarkar, V. S. Moholkar, *International Journal of Research in Engineering and Technology* **2**, 177 (2013).
- [21] M. Ahmad, E. Ahmed, Z. L. Hong, N. R. Khalid, Ahmed, W. A. Elhissi, *Journal of Alloys and Compounds* **577**, 717 (2013).
- [22] A. N. Mallika, A. Ramachandra Reddy, K. SowriBabu, Ch. Sujatha, K. Venugopal Reddy, *Optical Materials* **36**, 879 (2014).
- [23] Y. Wang, J. Liu, L. Liu, D. D. Sun, *Journal of Nanoscience and Nanotechnology* **12**, 1 (2012).
- [24] Q. Shi, J. Zhang, D. Zhang, C. Wang, B. Yang, B. Zhang, W. Wang, *Materials Science and Engineering B* **177**, 689 (2012).
- [25] F. Shabnam, M. Jamzad, H. K. Fard, *Green Chemistry Letters and Reviews* **12**(1), 19 (2019).